Polymer 50 (2009) 1732–1742

Contents lists available at ScienceDirect

Polymer

journal homepage: www.elsevier.com/locate/polymer

Crystallization and final morphology of HDPE: Effect of the high energy ball milling and the presence of TiO_2 nanoparticles

D. Olmos [a], C. Domínguez [b], P.D. Castrillo [a], J. Gonzalez-Benito [a,*]

[a] Dpto. de Ciencia e Ingeniería de Materiales e Ingeniería Química, Universidad Carlos III de Madrid, Avda Universidad 30, 28911 Leganés, Spain
[b] LATEP-GIQA, Universidad Rey Juan Carlos, 28933 Móstoles, Spain

ARTICLE INFO

Article history:
Received 1 October 2008
Received in revised form
1 February 2009
Accepted 4 February 2009
Available online 20 February 2009

Keywords:
Nanocomposites
Polyethylene
AFM

ABSTRACT

The influence of high energy ball milling process, HEBM, and the presence of TiO_2 nanoparticles on the non-isothermal crystallization and fusion behavior of the HDPE were investigated. HEBM was used to homogeneously disperse TiO_2 nanoparticles into a high density polyethylene, HDPE. Differential scanning calorimetry was used to analyze their non-isothermal crystallization and fusion behavior while, with X-ray diffraction the crystalline structures were determined. Atomic force microscopy was used to study the influence of the presence of nanoparticles on the final morphology of the polymer. It has been demonstrated that HEBM is a good method to prepare nanocomposites of well dispersed TiO_2 nanoparticles within an HDPE matrix. When nanoparticles are absent the HEBM induces reduction of crystallinity of the polymer although a double crystallization process was observed; however, when nanoparticles are present, in addition of being favored the appearance of a metastable monoclinic phase, the fraction of crystals increases as milling time increases. AFM clearly showed how well dispersed were the TiO_2 nanoparticles within the HDPE and how they are localized exactly between the lamellas. This result is the first clear visual evidence confirming that well dispersed nanoparticles actually do not act as nucleating agents in semicrystalline polymers. It was also shown that a 2% by weight of well dispersed TiO_2 nanoparticles within the HDPE matrix induces a more homogeneous crystallization leading to denser spherulites with thicker lamellae.

1. Introduction

Polymers filled with inorganic nanoparticles are a very important sort of nanocomposites based on the use of a polymer matrix. They usually combine the advantages of a polymeric matrix with the unique characteristics of the inorganic nanoparticles. The incorporation of certain nanoparticles makes the nanocomposites to gain a series of unique properties, such as optical, electrical, magnetic, surface wear properties, etc.

However, in general there is a high tendency of nanoparticles within polymer matrices to separate into discrete phases with agglomeration. This result usually leads to poor mechanical and optical properties of the composite [1]. Therefore, it is generally accepted that to achieve optimal enhancement of properties, the particles must be uniformly dispersed within the polymer matrix. To overcome this, different strategies have been considered, for example: melt processing [2,3], chemical modification of the nanoparticle surface [4–6]; chemical modification of the polymer matrix generating specific functional groups [7]; in situ polymerization, dispersing the nanoparticles in a monomer and then polymerizing the mixture [8] and nanoparticle creation within the polymer matrix by means of conventional sol–gel methods [9]. In general, these methods rely on processing the materials in melt or in solution, therefore using relatively high temperature or solvents. However, they do not seem to ensure a homogeneous dispersion of nanoparticles when the load of the filling material is higher than 5% by weight.

Recently, "solid state methods" such as high energy blending by ball milling have been proved to be an alternative method to achieve good dispersion of nanoparticles into thermoplastic polymers avoiding to work at high temperatures and/or with solvents [10–12]. Because of this, more work should be done taking into account this mixing process to finally understand which exactly the mechanism is causing such a good dispersion of nanoparticles.

Studying silica nanoparticles/PMMA nanocomposites Gonzalez-Benito [13] has demonstrated by FTIR that HEBM induces particular conformational changes on both the ester group and the

* Corresponding author. Tel.: +34 91 624 8870; fax: +34 91 624 9430.
E-mail address: javid@ing.uc3m.es (J. Gonzalez-Benito).

0032-3861/$ – see front matter © 2009 Elsevier Ltd. All rights reserved.
doi:10.1016/j.polymer.2009.02.011

backbone of the PMMA, which seems to be the cause of subsequent appearance of specific polymer chain packing at the interface. However, depending on the conditions selected this process may alter the polymer and because of this, to understand the effect of milling process on the structure and morphology of the polymers is necessary to adequately control the properties of the final material.

When a semicrystalline polymer is modified by nanoparticles, apart from obtaining unique properties due to the self-presence of the nanoparticles, they can lead to improved or modified properties because of its influence on the final polymer morphology. Therefore, when inorganic nanoparticles are mixed with the polymer by HEBM especial attention should be paid.

Compared with the isothermal crystallization conditions, the non-isothermal crystallization conditions are much closer to the real industrial processing conditions (extrusion, injection molding, and film blowing) and the results of investigation on non-isothermal crystallization should guide better to control the structure of the final material.

In crystalline polymers several properties are highly affected by the crystallinity because of both aspects: (i) the degree of crystallinity and (ii) the morphology (crystal sizes and crystalline structure). Examples are the hardness, yielding, optical and electrical properties, etc. On the other hand; it is well known that the properties of semicrystalline polymers greatly depend on the number, size and organization of the crystals which, in addition, depend on the conditions under which the crystallization process is carried out. Therefore, to understand the kinetics of this process is a prerequisite to be able to control the properties of those polymers.

In particular, in the case of nanocomposites, understanding the influence of the filler surface on the crystallization of polymers is important for tailoring the properties of polymer composites [14]. The best known effects which were observed are heterogeneous nucleation, transcrystallinity and epitaxy [15–18]. According to the classical approach solid surfaces present in a polymer melt induce heterogeneous nucleation due to reduced critical enthalpy for nucleation at the melt/solid interface [19]. At the molecular level, simulation and some experimental results show that in the vicinity of a solid wall chain configuration and even mobility is different as compared to bulk melt. At the solid surface a preferential orientation, elongation and flattening of polymer coil are observed in experiments [20,21] and in simulations [22–25]. Therefore, this particular influence must have a clear effect on the crystallization process and final morphology of the polymer close to solid particles.

The effect of solid micro- or nanoparticles on polymer crystallization can relatively easily be investigated in calorimetric studies [26,27]. However, much more difficult is to study the polymer structure and morphology in the vicinity of the polymer/filler interface. The investigations of morphology of the polymer layer crystallized in contact with a solid are particularly difficult when microscopic or nanoscopic solid particles are in play and, due to this, much more effort should be focused to this issue in order to understand the calorimetric results and mainly the final properties and performance of the nanocomposites.

In this work neat high density polyethylene, HDPE, and HDPE/TiO_2 nanocomposites obtained after blending HDPE and titanium dioxide nanoparticles (TiO_2) by HEBM process have been studied. They were analyzed using differential scanning calorimeter (DSC), X-ray diffraction and AFM to examine the influences of a process of high energy ball milling and the presence of TiO_2 nanoparticles on the crystallinity, morphology and the polyethylene non-isothermal crystallization and fusion behavior.

2. Experimental section

2.1. Materials

The HDPE (melt index at 190 °C/2.16 kg is 1.8–3.2 g/10 min) was supplied as pellets by Dow Chemical Co. (Dow Europe GmbH). The TiO_2 nanoparticles with a mean diameter of 65 nm were supplied by Aldrich.

2.2. High energy ball milling, HEBM

HDPE pellets were firstly grinded in an MF 10 basic Microfine grinder drive (IKA WERKE) to obtain relatively fine HDPE particles. After that, the HDPE particles were mixed with the titanium dioxide nanoparticles in a weight proportion of 2% of TiO_2. Subsequently, about 20 g of the mixture were introduced in a vial of alumina together with 190 g of alumina balls with 20 mm of diameter. The vial was then hermetically closed and placed in a Pulverisette 5 Fritsch apparatus where the powder was milled (400 rpm) for 10 h at room temperature (high energy ball milling, HEBM). To study the effect of the milling time on the blending process, samples of titania–HDPE were extracted at different milling times (1, 2, 4, 8 and 10 h) leaving the equipment to rest 25 min every hour of active milling. On the other hand, to avoid excessive heating of the equipment, as well as of the milled powders, a sub-cycle of milling was considered. Every 15 min of active milling was followed by 3 min of resting. For later comparisons pure HDPE was subjected to the same ball milling cycles.

2.3. Size exclusion chromatography, SEC

High temperature Waters Alliance GPCV 2000 SEC (size exclusion chromatography) equipped with refractometer and viscometer detectors was used to obtain molecular weight and molecular weight distribution of the samples. The molecular exclusion was made by three columns, two Plgel 10 mm Mixed-B and one 10 mm 10^6 Å. 1,2,4-Trichlorobenzene (TCB) was used as solvent at 145 °C and the flow rate was 1.0 ml/min. The instrument was previously calibrated with narrow standard polystyrene samples, according to the universal calibration method.

2.4. Differential scanning calorimetry, DSC

The non-isothermal crystallization behavior of the pure HDPE and its nanocomposites was analyzed using a Metler Toledo 822E differential scanning calorimeter. The temperature scale of the DSC was calibrated from the melting point (156.60 °C) of high purity (99.999%) indium metal. The power response of the calorimeter was calibrated from the enthalpy of fusion of indium (28.45 J/g). All DSC analyses were performed under nitrogen atmosphere.

Two groups of samples were considered: the first one corresponding to the neat HDPE milled for different milling times and the other to the HDPE/TiO_2 nanocomposites obtained at different milling times. All the experiments were conducted as follow. First of all, the samples were heated from 40 °C to 180 °C at 10 °C/min and the temperature was maintained at 180 °C for 5 min to erase the thermal history of the samples. Secondly, the samples were cooled at 10 °C/min from 180 °C to 40 °C to study the crystallization process at this cooling rate. After that, the samples were maintained at 40 °C for 5 min and finally they were heated at 10 °C/min from 40 °C to 180 °C to study the melting process of HDPE. The exothermic and endothermic curves were recorded for subsequent analysis.

Heating scans were analyzed in terms of the initial melting temperature, T_{mi}, the peak, T_{mp}, the final melting temperature, T_{mf},

and the heat of fusion, ΔH_m, while cooling scans were used to obtain the initial crystallization temperature, T_{ci}, the peak or peaks (depending on the case) crystallization temperatures, T_{cp}, the final crystallization temperature, T_{cf}, and the heat of crystallization, ΔH_c. The heat of fusion, ΔH_m, which was determined by integrating the heat flow from 90 °C to 140 °C, was used to calculate the degree of crystallinity, X_m, of HDPE on both the neat HDPE and HDPE/TiO_2 nanocomposites. X_m is defined by the ratio between $\Delta H_m/(1-x)$ (where x is the content of TiO_2 nanoparticles) and the heat of fusion of the purely crystalline form of PE, $\Delta H_m^\circ = 289.9$ J/g [28].

$$X_m = \frac{\Delta H_m/(1-x)}{\Delta H_m^\circ} \quad (1)$$

It is important to remember that crystallization and melting occur at temperatures different from T_m° (temperature from which ΔH_m° is determined). In fact, the crystallization and melting occur dynamically but not isothermically so one should be very careful when interpreting data using thermodynamic magnitudes when kinetics aspects might play an important role on final results. In this sense it would be interesting to take into account the temperature dependence of ΔH_m considering for example the procedure suggested by V.B.F. Mathot [29]. However, the intention of the authors of this article has been only to compare results from different samples and therefore, at least, to extract semiquantitative conclusions from a degree of crystallinity considered as the crystallinity relative to the maximum that can be obtained for the polymer under study.

The heats of crystallization, ΔH_c, were determined by integrating the cooling scans from 70 °C to 130 °C. Fig. 1 shows a representative example of a full heating and cooling cycle and the analytical method used to calculate ΔH_m, ΔH_c, T_{mi}, T_{mp}, T_{mf}, T_{ci}, T_{cp}, and T_{cf}.

2.5. Atomic force microscopy

Atomic force microscopy (AFM) studies were performed with a scanning probe microscope MultiMode Nanoscope IVA (Digital Instruments/Veeco Metrology Group). All measurements were carried out at ambient conditions in tapping mode with etched silicon probes (stiffness 40 N/m). The driving frequency of the probe was adjusted to the resonant frequency in the immediate vicinity of the samples.

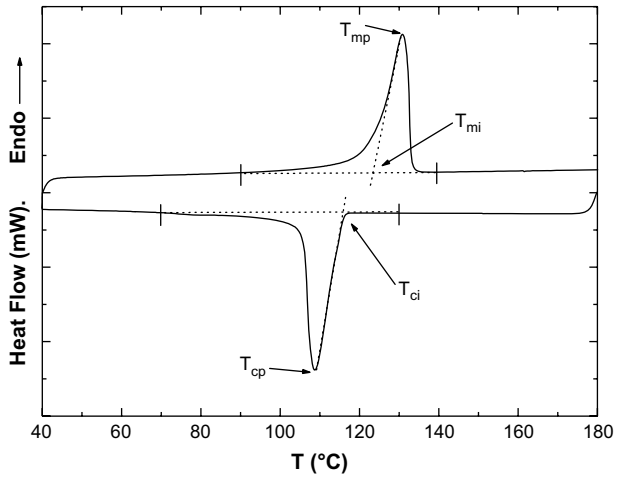

Fig. 1. DSC trace obtained from a representative example of a full heating and cooling cycle (neat HDPE). Some analytical parameters used in this work are also shown: T_{mi}, T_{mp}, T_{ci}, and T_{cp} (see text).

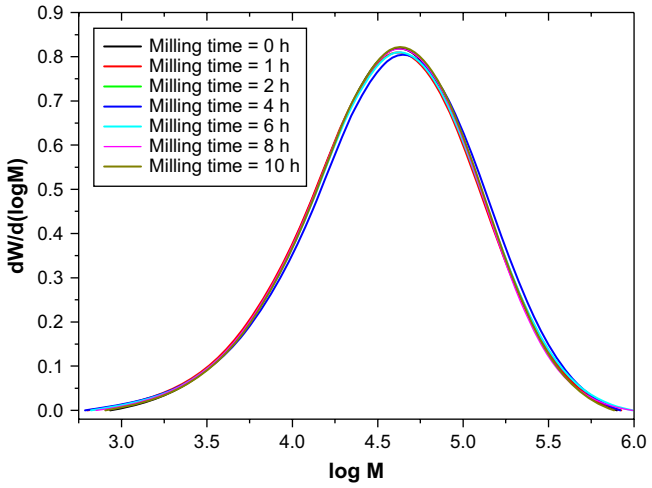

Fig. 2. Molecular weights distribution obtained for the sampled of HDPE milled for different times.

3. Results and discussion

3.1. Influence of HEBM on the molecular weight of the HDPE

All the chromatograms obtained by SEC shown a monomodal distribution of molecular weights as those presented in Fig. 2. On the other hand, in Table 1 are gathered all of the data obtained from the molecular weight distributions of the neat HDPE milled at different times. As can be observed there is not any significant change in the molecular weight distribution, being the variation of the molecular weight parameters below 5%. This change is within the representative variability associated to the SEC analysis which indicates no changes in the molecular weight distribution. Therefore, at the sight of these results, neither chain scission nor reticulation process seems to take place.

In the case of other polymers like PMMA, a clear change in the average molecular weight was observed when they are subjected to the same milling process. That result was assigned to scission of macromolecular chains [13]. Therefore, in the case of this HDPE the process of HEBM does not seem to alter the length of the polymer chains.

3.2. Influence HEBM on non-isothermal crystallization and melting behavior

The non-isothermal crystallization curves of the neat HDPE subjected to an HEBM process for different milling times are represented in Fig. 3. It can be clearly observed how the milling process exerts an important effect on the crystallization behavior of the HDPE (Fig. 3). It is observed how a new peak appears centered at

Table 1
Data extracted from the molecular weight distributions of the neat HDPE milled at different times.

Sample	Milling time (h)	M_n (g/mol)	M_w (g/mol)	M_z (g/mol)	M_{z+1} (g/mol)	Polydispersity
PE-0	0	19,284	65,864	1,58,932	2,74,397	3.4
PE-1	1	18,069	65,340	1,60,539	2,81,350	3.6
PE-2	2	18,072	66,917	1,71,976	3,16,037	3.7
PE-4	4	18,682	69,275	1,67,407	2,87,069	3.7
PE-6	6	18,594	67,768	1,71,894	3,12,449	3.6
PE-8	8	18,676	65,348	1,61,737	2,95,257	3.5
PE-10	10	19,314	65,342	1,53,798	2,62,360	3.4

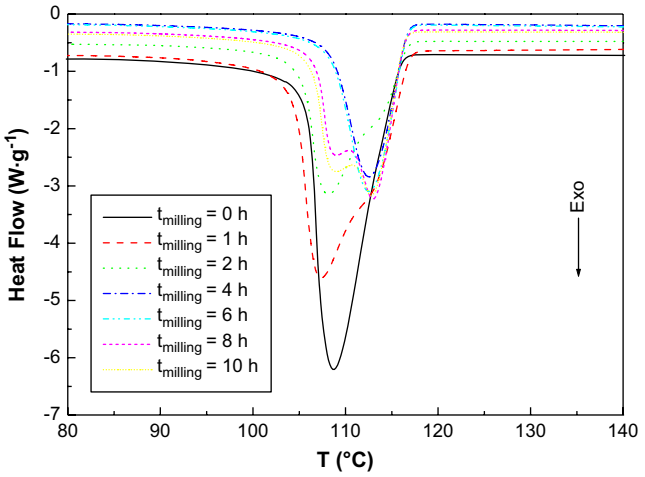

Fig. 3. Non-isothermal crystallization curves of the neat HDPE milled for different times.

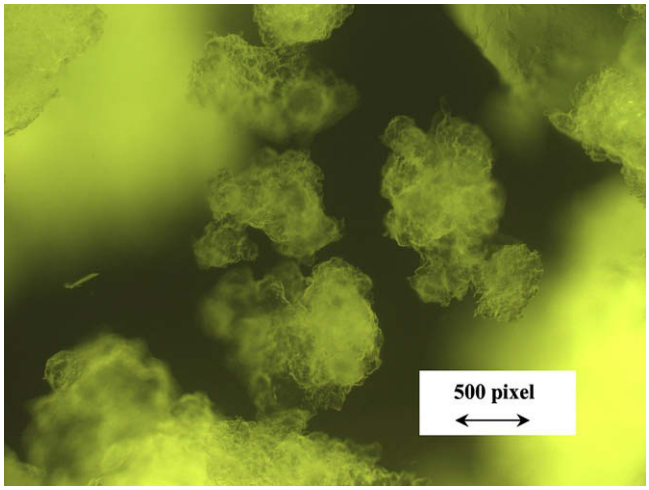

Fig. 4. Image representing the flake-like shape of the HDPE after more than 2 h of milling (the image was obtained making use of an LSM 5 PASCAL microscope of Zeiss taking the photo with an Axiocam HRC camera of Zeiss). 10 pixel ↔ 3.2 μm.

about 113 °C. Besides, this peak increases but only until the time of 8 h of milling. At this time, the relative contribution of the new peak starts to level off or even to slightly decrease. The values of ΔH_c, T_{ci}, T_{cp}, T_{cp2} (second crystallization temperature appearing with milling) and X_C are listed in Table 2. It is observed how the degree of crystallinity obtained from the cooling scans, X_C, decreases with milling time, going from about an 80% of crystals when the polymer is not milled to about a 50% when the HDPE is milled for 2 h. Therefore, although the milling induces a double crystallization process, being the first one different than that observed for the unprocessed polymer, the fraction of crystals is lower.

Apparently, taking into account the molecular weight distributions obtained by SEC, the HDPE has not suffered any molecular change. The data of the Table 1 point out that there had not neither chain scission nor a reticulation process provoked by the HEBM process. Therefore, other must be the cause that leads to a new crystallization process at higher temperature. Now it is interesting to mention that the results of Fig. 3 and Table 2 are in accordance with those reported by Castricum et al. [30] and Ishida [31] respectively. Ishida [31] reported that mechanical milling of pure polymer induces amorphization (mechanical milling leads to lower fraction of crystals). On the other hand, Castricum et al. [30] clearly showed that under certain conditions of mechanical milling crystalline polyethylene is transformed from the orthorhombic to the monoclinic structure (double crystallization). Furthermore, when powders of polymer are obtained at any milling condition the transformation was partial, while when a flake-like form is obtained for the final particles of milled polymer a complete transformation is obtained [30]. This is, in fact, the particle shape obtained in this work (flake-like) under the conditions of milling used in this work (see Fig. 4). Thus, important transformation from the orthorhombic to the monoclinic structure is expected if the results of Fig. 3 and the aspect shown by the milled polymer (Fig. 4) are taken into consideration.

However, Castricum et al. [30] reported that no detectable changes occurred in DSC in any of the samples they studied and, after melting, the material became orthorhombic again. This result which is the expected one if melting erased any preferential conformation acquired due to the important shear forces imposed by the milling process does not seem to be supported by the DSC traces of Fig. 3. Now is important to highlight that Castricum et al. [30] did not give any experimental detail about DSC scans; therefore, a possible explanation of the results obtained may be to consider that at 180 °C, 5 min is not time enough to forget the particular chain alignment induced by the milling process and which might be the germ of the metastable monoclinic phase of polyethylene.

In order to clarify this apparent contradiction, X-ray diffraction experiments were carried out for samples milled for 10 h with different thermal treatment. Fig. 5 shows the diffraction patterns of

Table 2
Values of the crystallization parameters ΔH_c, T_{ci}, T_{cp}, and T_{cp2} (see text).

Sample	Milling time (h)	T_{ci} (°C)	T_{cp} (°C)	T_{cp2} (°C)	ΔH_c (J/g)	X_C
PE-0	0	115.1	108.6	–	−227.8	0.79
PE-1	1	116.9	107.4	113	−216.8	0.75
PE-2	2	116.7	108.2	113	−133.0	0.46
PE-4	4	116.8	108.6	113	−188.5	0.65
PE-8	8	113.9	109.5	113.0	−136.0	0.47
PE-10	10	113.7	109.9	113.0	−143.6	0.50
PE/TiO_2-1	1	117.1	108.6	113	−167.4	0.58
PE/TiO_2-2	2	116.9	108.9	113	−147.6	0.51
PE/TiO_2-4	4	116.6	109.3	113	−201.4	0.69
PE/TiO_2-8	8	116.6	–	113.0	−194.7	0.65
PE/TiO_2-10	10	116.7	–	113.0	−216.0	0.75

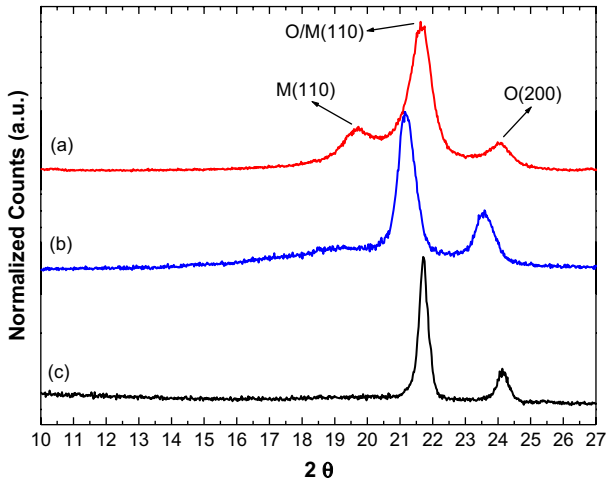

Fig. 5. Diffraction patterns of HDPE milled for 10 h: a) without further thermal treatment; b) heated at 180 °C for 5 min and cooled inside the oven and c) heated at 180 °C for 1 h and cooled in the oven.

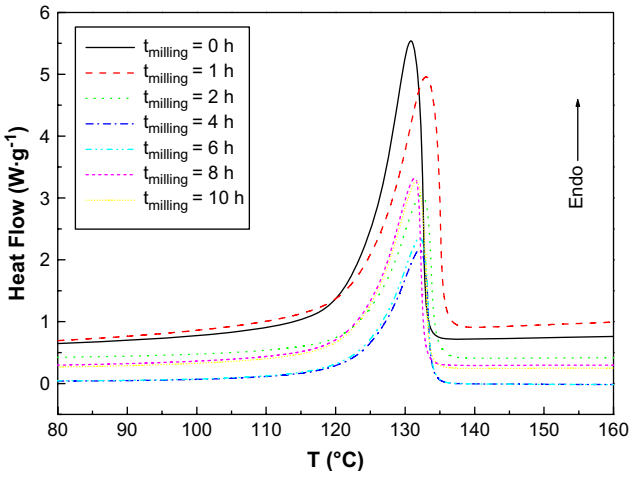

Fig. 6. Non-isothermal melting curves of the neat HDPE milled for different times.

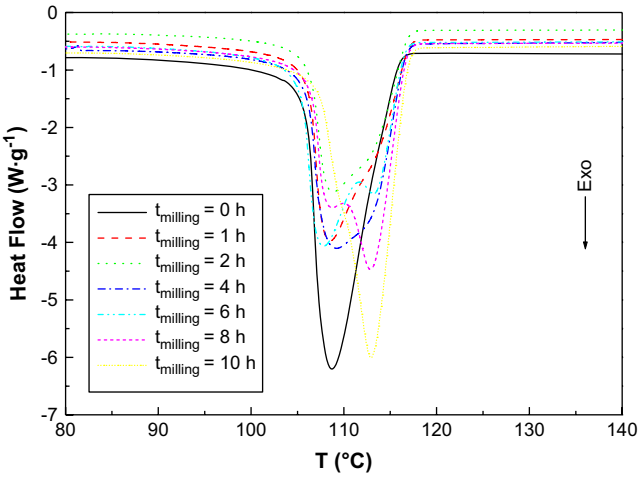

Fig. 7. Non-isothermal crystallization curves of the HDPE blended with TiO_2 nanoparticles milled for different times.

the HDPE milled for 10 h. On top of Fig. 5 is represented the diffraction pattern of the sample milled without any subsequent thermal treatment; in the middle of Fig. 5 is shown the diffraction pattern of the same sample but heated at 180 °C for 5 min and cooled inside the oven (trying to simulate the conditions of DSC cooling curve of Fig. 3) and finally, at the bottom of Fig. 5 the diffraction pattern of the same sample heated at 140 °C for 1 h and cooled in the oven is represented. It is observed, in complete agreement with Castricum et al. [30] that the milled sample without thermal treatment (Fig. 5a) shows the monoclinic ($\bar{1}10$) peak (M) together with the (110) and (200) peaks assigned to the orthorhombic structure (O), while the milled sample heated well above the melting point for long enough time does not show the monoclinic phase (Fig. 5c). However, when the thermal treatment above the melting point is not long enough, the polymer can crystallize in certain extension in the metastable monoclinic phase (Fig. 5b). These results suggest therefore that the second crystallization observed by DSC (Fig. 3) must belong to the formation of the metastable monoclinic phase and that is due to the previous heating treatment was not enough to erase the specific chains conformation or packing generated by the HEBM process. This result is interesting since as a function of milling probably, with this powder of milled polymer, in certain conditions of processing one could obtain materials with different properties associated to different crystalline structures. The reason why the peaks do not appear at the same position for the three samples must be attributed to the irregular shape of the sample to be tested by XRD.

The non-isothermal melting curves of HDPE milled for different times are represented in Fig. 6. None important change is observed with the milling process, perhaps only a small peak appears shifted to higher temperatures. The values of ΔH_m, T_{mi}, T_{mp}, and X_m are listed in Table 3. As expected, the degrees of crystallinity obtained from the melting curves (Fig. 6 and Table 3), X_m, are highly coincident with those obtained from the crystallization curves (Fig. 3 and Table 2), X_c: therefore, melting traces also point out that milling process induces reduction of crystallinity of the polymer. Besides, only one melting peak is observed suggesting that the whole melting comes from the two crystalline phases obtained after crystallization. A possible explanation of this result might be to consider that during the heating scan the orthorhombic phase changes to the monoclinic before melting with very low energy consumption.

Table 3
Values of the melting parameters ΔH_m, T_{mi}, T_{mp}, and X_m (see text).

Sample	Milling time (h)	T_{mi} (°C)	T_{mp} (°C)	<T_m> (°C)	ΔH_m (J/g)	X_m
PE-0	0	123.7	130.8	126.5	226.8	0.78
PE-1	1	124.7	133.0	135.1	223.1	0.77
PE-2	2	124.4	132.3	129.3	137.4	0.47
PE-4	4	124.3	132.1	127.6	186.8	0.62
PE-8	8	123.8	131.3	127.7	134.8	0.46
PE-10	10	123.8	131.7	126.3	143.3	0.49
PE/TiO_2-1	1	123.4	130.8	126.2	167.6	0.58
PE/TiO_2-2	2	124.4	132.4	128.3	144.1	0.50
PE/TiO_2-4	4	124.0	132.0	127.5	194.5	0.67
PE/TiO_2-8	8	123.8	131.7	126.9	191.0	0.66
PE/TiO_2-10	10	124.5	131.3	126.6	205.5	0.71

3.3. *Influence of the presence of TiO_2 nanoparticles on the non-isothermal crystallization and the melting behavior*

The non-isothermal crystallization and melting curves of the HDPE blended with TiO_2 nanoparticles (PE/TiO_2) and subjected to different milling times are represented in Figs. 7 and 8 respectively. Although now more pronounced, the milling process exerts over the crystallization process (Fig. 7) the same effect than in the case of

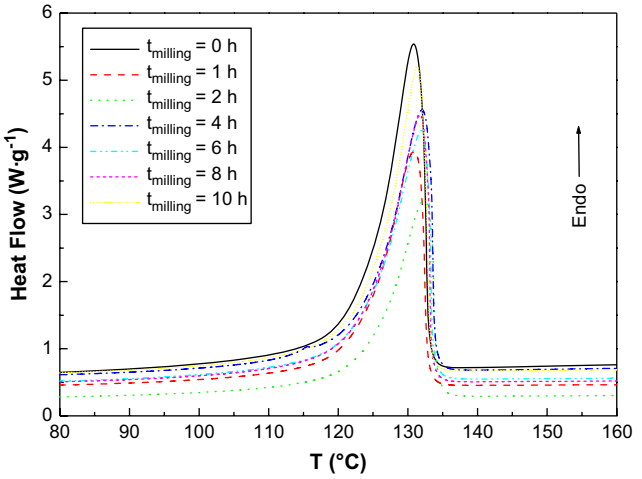

Fig. 8. Non-isothermal melting curves of the HDPE blended with TiO_2 nanoparticles subjected at different milling times.

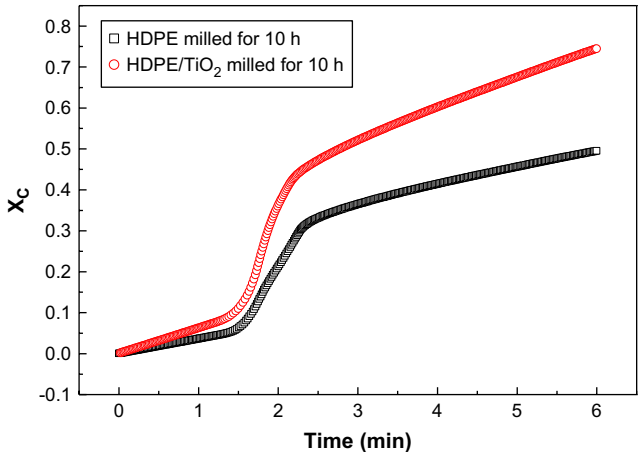

Fig. 9. Degree of crystallization as a function of time obtained from the non-isothermal experiment for two kinds of samples, neat HDPE milled for 10 h and HDPE/TiO_2 nanoparticles milled for 10 h.

the neat HDPE (without nanoparticles). On the other hand, the melting curves (Fig. 8) do not show significant differences respect to those of the neat HDPE. The thermal parameters related to the crystallization and melting process (values of ΔH_c, T_{ci}, T_{cp}, T_{cp2}, X_C and the values of ΔH_m, T_{mi}, T_{mp}, X_m) are listed in Tables 2 and 3 respectively. It can be seen that although the position of the peaks do not differ from those observed for the neat HDPE there is an important difference when the nanoparticles are blended with the HDPE; the degree of crystallinity increases with milling time, going from about a 60% of crystals when the mixture is milled for 1 h to about a 70% when the mixture is milled for 10 h. It is clear therefore that the presence of the nanoparticles favors the formation of crystals. This result is also important because the nanoparticles, apart from giving intrinsically specific properties to the final nanocomposites, can induce changes in the nanocomposite properties due to changes in the polymer morphology. On the other hand, the higher crystallinity values should enhance critical mechanical properties such as stiffness and impact resistance, improving the nanocomposite properties.

3.4. Non-isothermal crystallization kinetics

In the process of non-isothermal crystallization, the temperature of the system during cooling can be converted into the corresponding crystallization time, t, as follows:

$$t = \frac{T_0 - T}{\phi} \tag{2}$$

where T_0 is the temperature for which the crystallization is considered to start ($t = 0$ s), T is the temperature for the crystallization time t and ϕ the cooling rate. As a consequence of this, the degree of crystallinity X_C as a function of crystallization time for the neat HDPE and HDPE/TiO_2 nanocomposites at various milling times can be obtained.

The effect of the TiO_2 nanoparticles in the crystallization rate can be clearly observed in Fig. 9. As an example it is shown the crystallization degree as a function of time obtained from the non-isothermal experiment for two kinds of samples, neat HDPE milled for 10 h and HDPE/TiO_2 nanoparticles milled for 10 h. The crystallization rate of the HDPE/TiO_2 nanocomposites has been found to be invariably faster than that of the neat HDPE. The reason of this behavior might be the very dramatic increase in the nucleation density in the melt of nanocomposites as it was observed in other

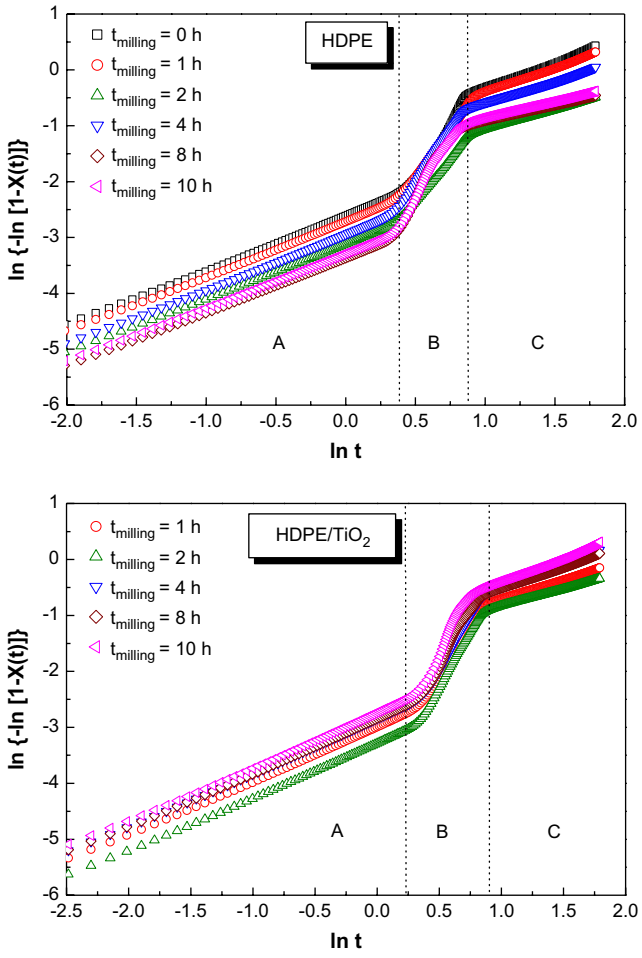

Fig. 10. Avrami's plots (crystallization time, t, in minutes) for the samples HDPE and HDPE/TiO_2 nanocomposites obtained at different milling times.

sort of nanocomposites [14,32]. However, other may be the reason if it is considered that well dispersed nanoparticles in a semi-crystalline polymer have not any nucleating effect as reported by Huang et al. [33] in the case of Al nanoparticles (average diameter of 50 nm) well dispersed in LDPE. The other possible explanation for this more rapid crystallization process may be a faster crystal growth when the nanoparticles are present since; in this case, the formation of metastable monoclinic phase is favored.

Once the data of crystallinity as a function of time is available, the kinetics analysis can be done making use of Avrami's equation

Table 4
Avrami's exponents obtained from the different regimes of the plots of Fig. 9.

Sample	n (Region A)	n (Region B)		n (Region C)
		Regime 1	Regime 2	
PE-0	0.91	4.14	–	0.93
PE-1	0.92	3.38	–	0.88
PE-2	0.91	3.10	–	0.71
PE-4	0.91	4.24	3.43	0.78
PE-8	0.91	5.44	2.98	0.56
PE-10	0.90	5.27	3.21	0.59
PE/TiO_2-1	0.91	3.57	–	0.68
PE/TiO_2-2	0.91	4.27	3.77	0.59
PE/TiO_2-4	0.92	4.17	3.68	0.82
PE/TiO_2-8	0.92	5.23	2.88	0.76
PE/TiO_2-10	0.92	5.96	2.80	0.86

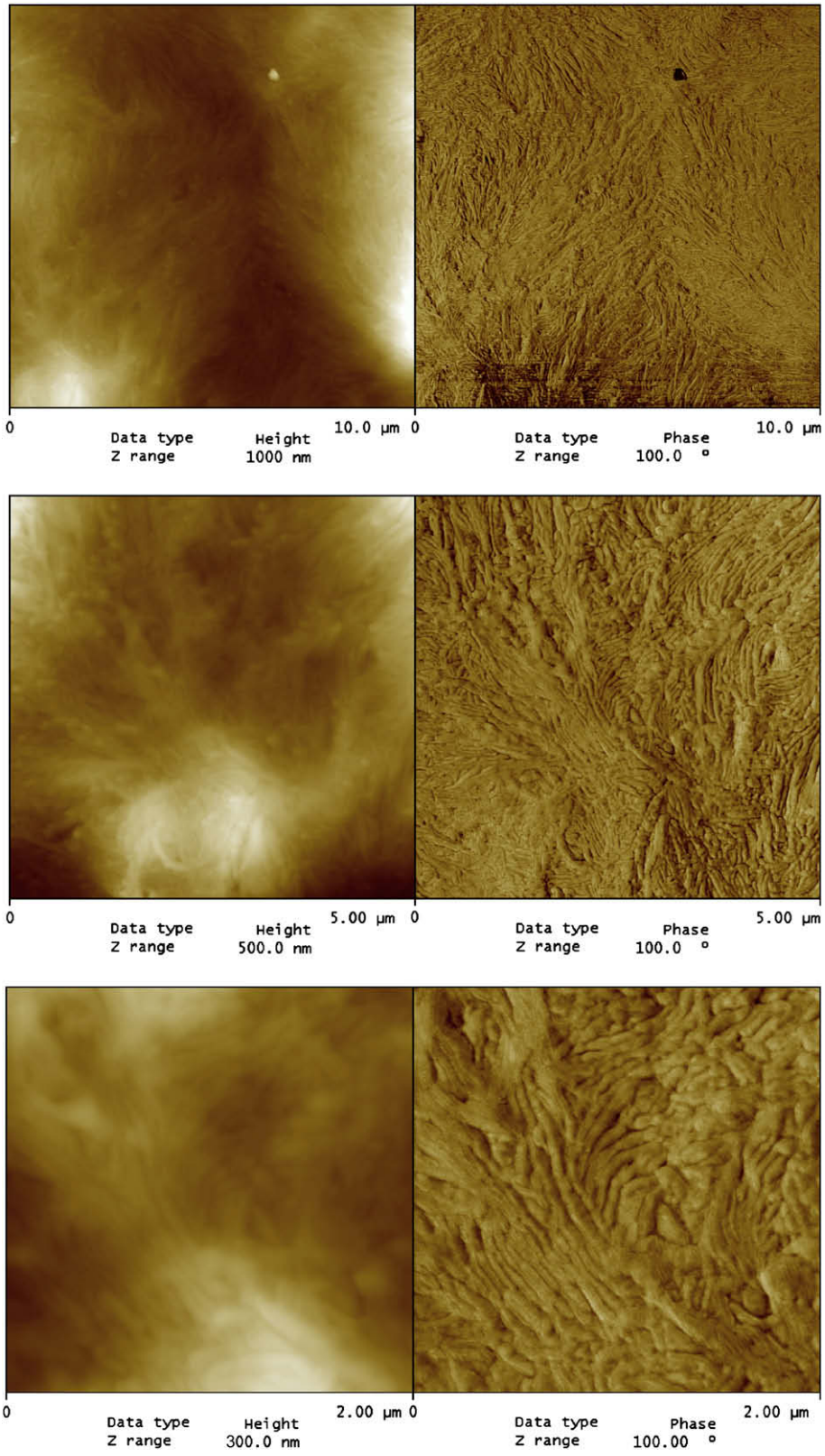

Fig. 11. Morphology of the HDPE milled for 10 h obtained by topographic and phase AFM images (left and right respectively).

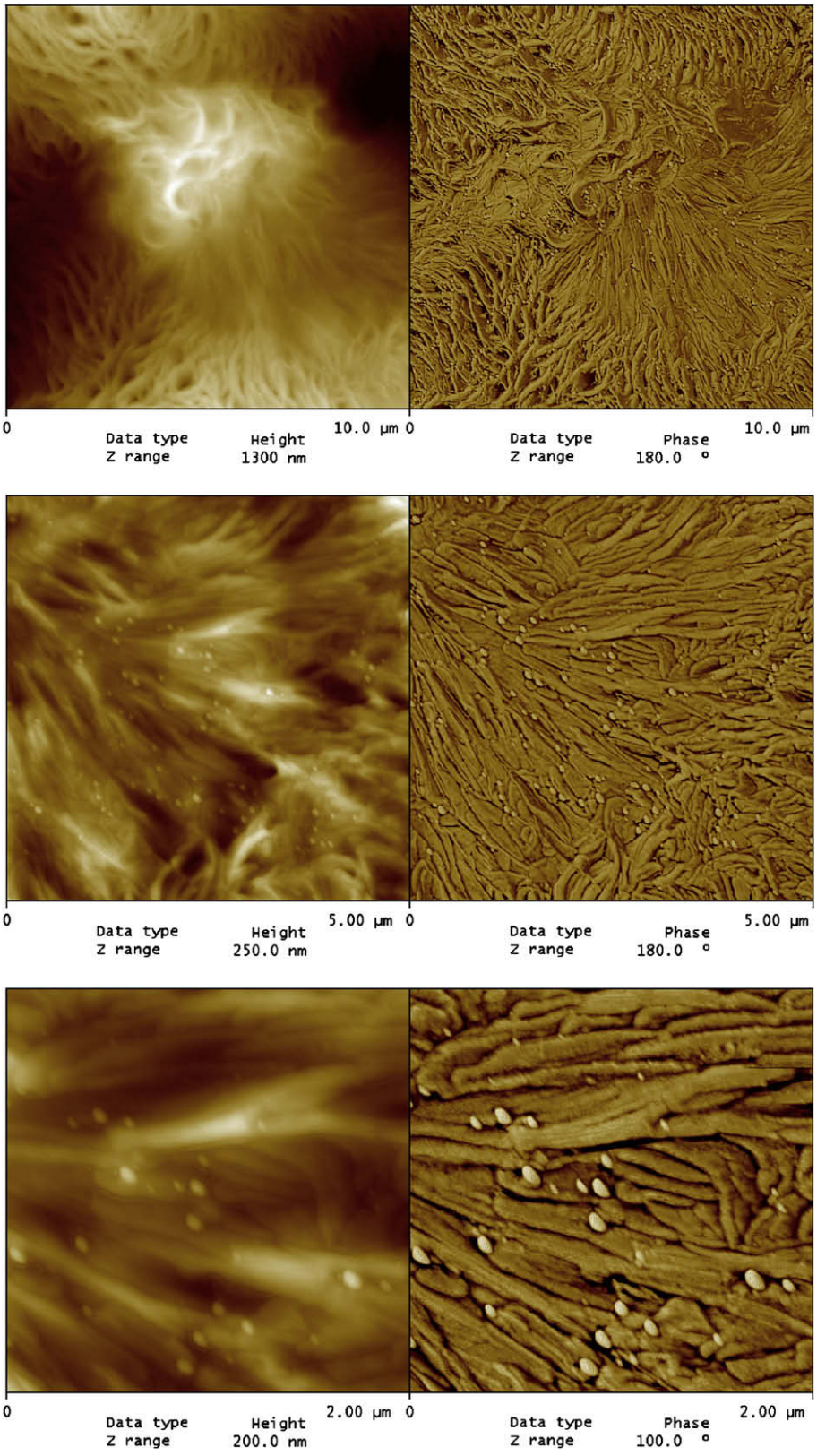

Fig. 12. Morphology of the HDPE/TiO_2 milled for 10 h obtained by topographic and phase AFM images (left and right respectively).

[34] modified by Jeziorny to describe the non-isothermal kinetics of polymers [35]:

$$1 - X(t) = \exp(-Z_t \cdot t^n) \quad (3)$$

where Avrami's exponent n is a constant that depends on the type of nucleation and growth process and Z_t is a rate constant involving both nucleation and growth rate parameters.

Taking double natural logarithms, the equation (3) is transformed into

$$\ln[-\ln(1 - X(t))] = \ln Z_t + n \cdot \ln t \quad (4)$$

Avrami's exponent n and the constant Z_t can be obtained respectively from the slope and the interception in the plot of $\ln[-\ln(1-X(t))]$ versus $\ln t$ at a certain cooling rate.

Avrami's plots for the samples HDPE and HDPE/TiO_2 nanocomposites milled for different times are shown in Fig. 10. Three regions (A, B and C in Fig. 10) can be observed which suggest three steps for the crystallization. In the region A the slopes of all plots indicate that the values of n are between 0.90 and 0.92 (Table 4), therefore, attending that n is related to the type of nucleation and growth process one might think in this case that for this material there is first a simple nucleation process which proceeds along the region A and when the region B is reached the crystals start to grow up. On the other hand, as can be seen in Table 4 the value of Avrami's exponent, n, obtained from the curves in the region B changes as a function of milling time and even though, in some cases, it can be split into two values because in the region B some curves present two regimes. In fact, what is observed is that for the region B, when milling time increases, n decreases until certain milling time for which the curve can be fitted to two straight lines leading therefore to two values of n. One of them, at shorter times of crystallization, which increases with milling time to values higher than 5 and, the other, at longer crystallization times, which remains between 3 and 3.4. These results suggest that the crystallization of the HDPE under study proceeds via a homogeneous nucleation and three dimensional growing when the polymer is not milled ($n = 3 + 1$ in region B) while when the HDPE is milled, two competing crystallization process must be taken into account. Considering the reduction of Avrami's exponent from 4 to 3 when milling time is increased from 0 h to 2 h, it is reasonable to think that at shorter milling times along the region B a heterogeneous nucleation with 3D growing of the orthorhombic phase occurs. In other words, the samples milled for shorter times under the conditions of our study only remain memory to generate, apart from orthorhombic crystals, nucleus of metastable monoclinic phase. Therefore, it is assumed that the heterogeneous nucleation is composed by the germ of the orthorhombic phase of the polymer and by the germ of the monoclinic phase. However, at higher milling times, the chain conformation is so forced that the polymer has memory enough as to yield double crystallization. The values of n higher than 5 (first regime of region B) would point out double crystallization, monoclinic plus orthorhombic, while the values of n near to 3 (second regime of Region B) would point out single orthorhombic crystallization process at the end of the whole crystallization.

Finally, in region C n ranges from 0.9 to 0.6, suggesting that, in the later stage, the crystals impinge on and crowd, the growth geometry of the crystal is then restricted and the crystals grow in lower dimension in this regime.

Although more pronounced, when TiO_2 nanoparticles are present within the HDPE similar results are obtained as a function of milling time. In this case, the nanoparticles seem to help remaining the memory of the metastable monoclinic phase. Therefore, the presence of TiO_2 nanoparticles favors the crystallization phenomena observed in the neat HDPE caused by the milling process. This result is in accordance with the consideration of a more restricted mobility of the polyethylene chains due to the presence of rigid nanoparticles well dispersed within the polymer and with a good contact between the nanoparticles and the polymer.

3.5. Morphological study: the effect of nanoparticles introduced by HEBM

In Figs. 11 and 12 the morphology of the milled materials for 10 h (Fig. 11 without nanoparticles and Fig. 12 with TiO_2 nanoparticles) is shown by means of topographic and phase AFM images (left and right respectively). Besides in each figure three magnifications were considered (10×10 μm top, 5×5 μm middle and 2×2 μm bottom) in order to evidence different details of the morphology. When lower magnification is considered it is possible to observe how despite the presence of nanoparticles the HDPE crystallizes in the form of the typical spherulites. However, for the sample with nanoparticles the spherulites seem to be denser

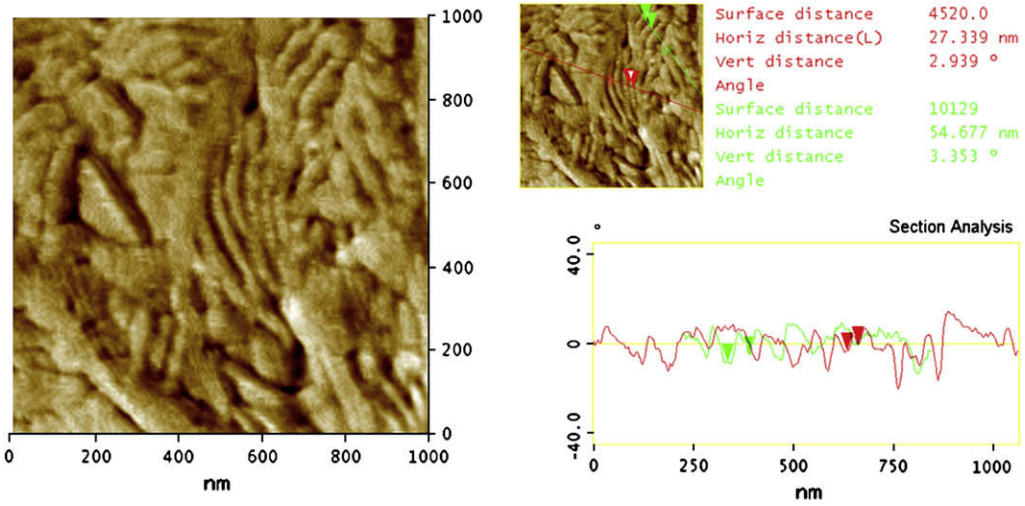

Fig. 13. Representative cross section profile measurements over the phase image of the neat HDPE.

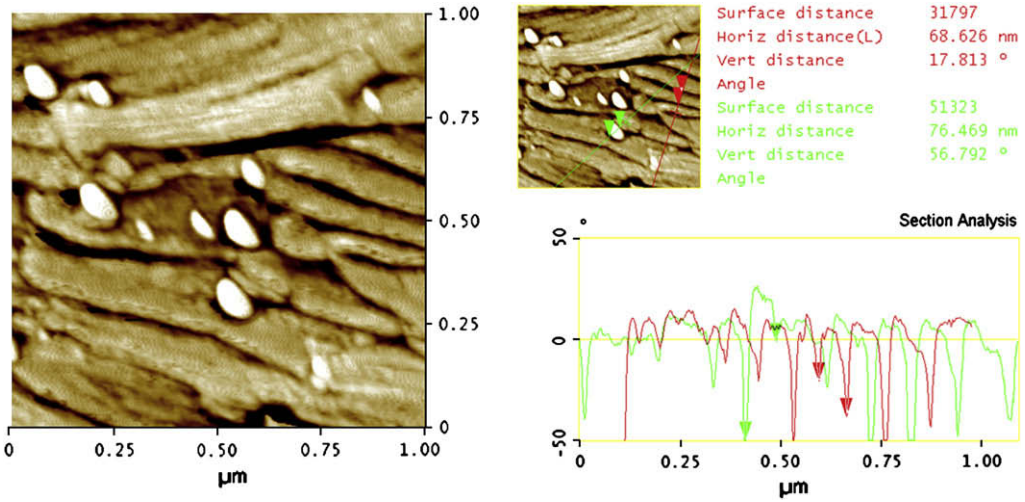

Fig. 14. Representative cross section profile measurements over the phase images of the HDPE/TiO_2 nanocomposite.

showing practically the total spherical form (Fig. 12 top), while in the case of neat HDPE it seems that the spherulites impinge before being completely formed (Fig. 11 top). Although the thermal treatment was different than that of the DSC scans, these results of morphology are in accordance with the degree of crystallinity obtained by DSC (last columns of Tables 2 and 3). The amount of crystals is clearly higher when the nanoparticles are present within the polymer.

On the other hand, the images at the middle and at the bottom of Figs. 11 and 12 clearly show how the presence of nanoparticles induces a more homogeneous crystallization. The lamellar structure is the same on the whole image when nanoparticles are present (Fig. 12) while, for the neat HDPE, groups of lamellas of different sizes can be observed (Fig. 11).

Figs. 13 and 14 show representative cross section profile measurements over the phase images of the neat HDPE and HDPE/TiO_2 nanocomposites respectively (measurements over topographic images gave the same results). It is observed that the HDPE milled for 10 h presents two groups of lamellas one of them whose thickness is about 27 nm and the other about 55 nm (Fig. 13). On the other hand, the HDPE/TiO_2 nanocomposite (sample milled for 10 h) only present a group of lamellas whose thickness is higher than 60 nm (Fig. 14). Besides, in Fig. 14 a representative measurement of a particle diameter is shown for which it was obtained a value of 76 nm, which is in the range of the specifications given by the nanoparticles supplier (diameters lower than 100 nm) and which guarantees the good observation of the nanoparticles in between lamellas.

Furthermore, the images of HDPE/TiO_2 nanoparticles (Fig. 12) clearly show the extraordinary nanoparticles dispersion attained with 10 h of HEBM. This result was furthermore reinforced after a bearing image treatment which yielded about 1.5% of the surface occupied by nanoparticles. This indicates that considering the density of the nanoparticles and HDPE $\sim 4\,g\,cm^{-3}$ and $\sim 1\,g\,cm^{-3}$ respectively, a weight fraction of about 0.06 (6% by weight) is expected. Taking into account that 2% by weight was the composition used in the mixture, the estimation performed slightly overestimates the amount of nanoparticles. However, as can be observed at the bottom of Fig. 12 the nanoparticles appear slightly distorted showing a kind of obloid shape. Therefore, if a spherical shape was considered the corrected fraction of nanoparticles would be lower than 1% by volume (or lower than 4% by weight) which is a result more than acceptable taking into account the difficulty of doing such a kind of analysis and the small regions that can be analyzed.

Another interesting observation is that the nanoparticles are placed exactly between the lamellas (Fig. 12 bottom) which evidences that they actually are not acting as nucleating agents as sometimes happen in polymers filled with well dispersed nanoparticles [33]. It seems that the nanoparticles follow the way of lamellar growing helping at the same time to yield more and more perfect crystals (structural changes of crystals) as also evidenced DSC results. It is generally accepted that the key factor for nucleating effect of fillers is their surface free energy and surface morphology [36]. Veseley [37] found that nucleating efficiency of the fillers is dependent on the size as well as on the crystallographic orientation of the facet, saying that only the large particles with well developed facets are nucleating, whereas the small particles or those with no suitable facets do not affect the crystalline structure of the polymer. However, it has been shown above that, at least for the system under study, the presence of TiO_2 nanoparticles modified the crystalline structure of the HDPE and therefore the second assertion of Veseley is not satisfied. Now it is time to be wondered if there is scale size limit for the nanoparticles (at nanoscale, sizes lower than 100 nm) in terms of inducing a particular morphology and this question only can be answered if a particular system is chosen and only the change in the size of the particles is investigated. This challenge is particularly difficult because of obtaining samples of monodisperse nanoparticles with sizes lower than 100 nm is not an easy task.

4. Conclusions

It has been demonstrated that HEBM is a good method to prepare nanocomposites of well dispersed TiO_2 nanoparticles within an HDPE matrix because, among other things, for this polymer neither chain scission nor reticulation process takes place. However, important changes in the crystalline structure and morphology were found because of both the HEBM process and the presence of the TiO_2 nanoparticles. It was observed that although in general there is a reduction of crystallinity of the polymer, when nanoparticles are absent the HEBM process induces a double crystallization process (appearance of both the orthorhombic and metastable monoclinic phases). However, when nanoparticles are present, in addition of being favored the appearance of the metastable monoclinic phase, the fraction of crystals increases as milling

time increases. AFM experiments have clearly shown how well dispersed are the TiO_2 nanoparticles within the HDPE and how they are localized exactly between the lamellas which evidences that they actually are not acting as nucleating agents. Besides, AFM images evidence that a 2% by weight of well dispersed TiO_2 nanoparticles within the HDPE matrix induces a more homogeneous crystallization leading to denser espherulites with thicker lamellae.

Acknowledgements

The authors gratefully acknowledge the MEC of Spain for financial support (project MAT2007-61607).

References

[1] Yang H, Zhang Q, Guo M, Wang C, Du NR, Fu Q. Polymer 2006;47(6):2106–15.
[2] Chandra A, Turng LS, Gopalan P, Rowell RM, Gong S. Compos Sci Technol 2008;68(3–4):768–76.
[3] Chandra A, Turng LS, Gong SQ, Hall DC, Caulfield DF, Yang HJ. Polym Compos 2007;28(2):241–50.
[4] Yang M, Dan Y. Colloid Polym Sci 2005;284(3):243–50.
[5] Rong MZ, Zhang MQ, Zheng YZ, Zeng HM, Walter R, Friedrich K. Polymer 2001;42(1):167–83.
[6] Ash BJ, Siegel RW, Schadler LS. Macromolecules 2004;37(4):1358–69.
[7] Bikiaris DN, Vassiliou A, Pavlidou E. Eur Polym J 2005;41(9):1965–78.
[8] Reynaud E, Jouen T, Gauthier C, Vigier G, Varlet J. Polymer 2001;42(21):8759–68.
[9] He J, Li H, Wang X, Gao Y. Eur Polym J 2006;42(5):1128–34.
[10] Gorrasi G, Sarno M, Bartolomeo A, Sannino D, Ciambelli P, Vittoria V. J Polym Sci Part B Polym Phys 2007;45(5):597–606.
[11] Castrillo PD, Olmos D, Amador DR, González-Benito J. J Colloid Interface Sci 2007;308(2):318–24.
[12] Castrillo PD, Olmos D, González-Benito J. J Appl Polym Sci 2009;111(4):2062–70.
[13] Gonzalez-Benito J, Gonzalez-Gaitano G. Macromolecules 2008;41(13):4777–85.
[14] Jeon K, Lumata L, Tokumoto T, Steven E, Brooks J, Alamo RG. Polymer 2007;48(16):4751–64.
[15] Sanchez IC. Physics of polymer surfaces and interfaces. Boston: Butterworth-Heineman; 1992.
[16] Wunderlich B. Macromolecular physics. New York: Academic Press; 1973.
[17] Thierry A, Mathieu C, Straupe C, Wittmann JC, Lotz B. Macromol Symp 2001;166(1):43–58.
[18] Billon N, Henaff V, Pelous E, Haudin JM. J Appl Polym Sci 2002;86(3):725–33.
[19] Wunderlich B. Crystal nucleation, growth, annealing. New York: Academic Press; 1976.
[20] Kraus J, Muller-Buschbaum P, Kuhlmann T, Schubert DW, Stamm M. Europhys Lett 2000;49(2):210–6.
[21] Jones RL, Kumar SK, Ho DL, Briber RM, Russell TP. Nature 1999;400:146–9.
[22] PaiPanandiker RS, Dorgan JR, Pakula T. Macromolecules 1997;30(20):6348–52.
[23] Pakula T. J Chem Phys 1991;95(6):4685–90.
[24] Baschnagel J, Meyer H, Varnik F, Metzger S, Aichele M, Muller M, et al. Interface Sci 2003;11(2):159–73.
[25] Meyer H, Baschnagel J. Eur Phys J E 2003;12(1):147–51.
[26] Jancar J, editor. In advances in polymer science, vol. Mineral Fillers in Thermoplastics I. Springer; 1999. p. 1–65 [chapter 1].
[27] Dollase T, Wilhelm M, Spiess HW, Yagen Y, Yerushalmi-Rozen R, Gottlieb M. Interface Sci 2003;11(2):199–209.
[28] Mandelkern L. Crystallization of polymers. In: Equilibrium concepts. 2nd ed., vol. 1. New York: Cambridge University Press; 2002. p. 259.
[29] Mathot VBF. Calorimetry and thermal analysis of polymers. In: Mathot VBF, editor. Thermal characterization of states of matter. Munich: Hanser Publishers; 1994. p. 103–67. chapter 5.
[30] Castricum HL, Yang H, Bakker H, Van Deursen JH. Mater Sci Forum 1997;235–238:211–6.
[31] Ishida TJ. Mater Sci Lett 1994;13(9):623–8.
[32] Haggenmueller R, Fischer JE, Winey KI. Macromolecules 2006;39(8):2964–71.
[33] Huang X, Ke Q, Chonung K, Zhong H, Wei P, Wang G, et al. Polym Eng Sci 2007;47(7):1052–61.
[34] Avrami M. J Chem Phys 1939;7:1103–12.
[35] Jeziorny A. Polymer 1978;19(10):1142–4.
[36] Tracz A, Kucinska I, Wostek-Wojciechowska D, Jeszka JK. Eur Polym J 2005;41(3):501–9.
[37] Vesely D, Ronca G. J Microsc Oxford 2001;201(part 2):137–43.